ELSEVIER

Surface Science 371 (1997) 53–62

surface science

Density functional study of acetylene and ethylene adsorption on Ni(111)

A. Fahmi *, R.A. van Santen

Schuit Institute of Catalysis, Laboratory of Inorganic Chemistry and Catalysis, Eindhoven University of Technology, P.O. Box 513, 5600 MB Eindhoven, The Netherlands

Received 18 March 1996; accepted for publication 19 July 1996

Abstract

Optimized geometries and adsorption energies obtained from non-local density functional calculations are presented for the adsorption of acetylene and ethylene on Ni(111). Two cluster models, Ni_4 and Ni_{14}, are used. The best adsorption modes are μ-bridging and di-σ for acetylene and ethylene, respectively. In these orientations the overlap between the adsorbate frontier orbitals and the metal cluster orbitals is important, and the donation and back-donation of electrons are large. The calculations support the picture of strongly distorted adsorbates on the surface.

Keywords: Alkenes; Alkynes; Chemisorption; Density functional calculations; Nickel; Single crystal surfaces

1. Introduction

Chemisorption of ethylene and acetylene on metal surfaces has been the subject of considerable interest. Many experimental as well as theoretical studies have been performed, mainly to gain insight in the geometrical and electronic aspects of the adsorption.

Both ethylene and acetylene adsorb molecularly on Ni(111) at 120 K [1] and the surface shows a p(2×2) LEED pattern [2–5]. Upon heating (165–240 K), ethylene decomposes into acetylene and atomic hydrogen [1]. At low coverage (<0.24 ML), temperature-programmed static secondary ion mass spectroscopy (TPSSIMS) experiments [1] have shown that the first step in acetylene decomposition is C–C bond cleavage. Methylidyne species (CH) were observed between 190 and 260 K. The C–H bond cleavage and the formation of acetylide species (C–CH) were observed at higher temperatures (260–350 K). The picture emerging from experiments on the nature of the adsorbate–metal bonding and the adsorbate geometry shows a significant rehybridization of both C_2H_2 and C_2H_4 molecules toward an sp^3 configuration [3,6]. Therefore the adsorbates are often described as di-σ bonded species, in contrast to π-bonded species which remain nearly unchanged upon adsorption. This terminology does not make any reference to the coordination of the adsorbates with the surface (number of metal atoms involved in the adsorption). In recent photoelectron diffraction experiments, Bradshaw and co-workers [7] determined the adsorption modes of both acetylene and ethylene on Ni(111): the

* Corresponding author. Fax: +31 40 2455054; e-mail: tgakaf@chem.tue.nl

PII S0039-6028(96)00974-0

coordination modes (Fig. 1) are suggested to involve four metal atoms for C_2H_2 (called the μ-bridging adsorption mode) and two metal atoms for C_2H_4 (also called the di-σ adsorption mode). On the other hand, LEED [9] and NEXAFS [10] experiments indicated that during the adsorption the C–C axis remains approximately parallel to the Ni(111) surface.

Theoretical cluster studies of acetylene adsorption on Ni(111) have utilized both semi-empirical (extended Huckel [11], CNDO [12]) and ab-initio (Hartree–Fock [13], X_α [8]) techniques. Other calculations concern Cu(111) (HF [14]), Pt(111) and Rh(111) (EHT [11,15]), and Pd(111) (HF [14]). For ethylene adsorption, the available results concern the adsorption on Ni(100) (X_α [16,17]) and Ni(110) (DFT [18]) surfaces. Other calculations concern the adsorption of ethylene on Pt(111) (EHT [19]) and Pt(110) (EHT [20]).

The picture emerging from these theoretical calculations shows the dependency of the adsorption mode on the surface of the metal: the C_2H_2 adsorption mode is μ-bridging on Ni(111) [8,13] and di-σ on Ni(110) [18]. For the same surface the adsorption mode depends on the coordination of the metal atoms involved in the interaction with the adsorbate: for C_2H_4/Pt(111), the di-σ mode is more stable on terraces, whereas the π mode is more stable on steps [19].

In this work, we present a density functional study of the molecular adsorption of acetylene and ethylene on Ni(111). We have used Ni_4 and Ni_{14} clusters as models for the metal surface. For each adsorbate, we compare the di-σ and μ-bridging adsorption modes. The geometries of the adsorbates are optimized with the Ni_4 cluster and transferred to the Ni_{14} cluster to obtain reliable adsorption energies. The method of calculation is presented in Section 2. The models for the adsorbate–substrate systems are discussed in Section 3. Section 4 concerns the bare clusters, and Sections 5 and 6 present the results of the adsorption of acetylene and ethylene, respectively.

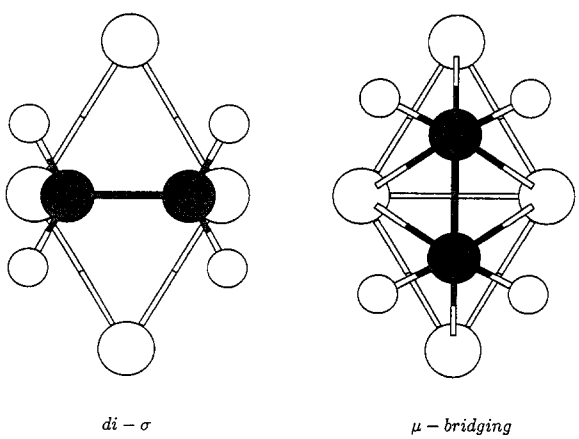

Fig. 1. Adsorption modes of ethylene: di-σ and μ-bridging.

2. Method of calculation

A density functional method is used to determine geometries and adsorption energies of C_2H_2 and C_2H_4 on Ni_4 and Ni_{14} clusters. We have performed quasi-relativistic spin-unrestricted, frozen-core calculations using the Amsterdam Density Functional (ADF) program [21]. The program represents the molecular orbitals as linear combinations of atomic Slater-type orbitals and solves the Kohn–Sham one-electron equations using the Vosko–Wilk–Nusair [22] local spin density approximation (LDA). To correct the overbinding inherent to LDA, non-local gradient corrections for the exchange (Becke functional [23]) and correlation (Perdew functional [24]) terms were computed self-consistently. Relativistic effects were taken into account by first-order perturbation theory [25]. Geometry optimizations have been performed within the non-local gradient correction by means of analytical gradient techniques, and the relativistic correction has been applied to the optimized geometries. For the carbon atom a frozen-core potential is used for the 1s electrons; for the nickel atom, electrons up to the 3p shell are frozen. The basis sets are of double-ζ quality, except the nickel d orbitals which are triple-ζ; on carbon and hydrogen atoms, polarization functions have been added.

Adsorption energies have been calculated according to the expression

$$E_{ads} = E_{cluster} + E_{adsorbate} - E_{(adsorbate/cluster)},$$

where $E_{cluster}$ and $E_{adsorbate}$ are total energies of the

bare cluster (Ni_4 or Ni_{14}) and the adsorbate (C_2H_2 or C_2H_4), respectively, and $E_{(adsorbate/cluster)}$ is the total energy of the adsorbate/substrate system. A positive E_{ads} value corresponds to a stable adsorbate/substrate system.

3. Model for the adsorbate/substrate system

Two metal clusters, Ni_4 and Ni_{14}, are used as models for the Ni(111) surface (Fig. 2). They are fragments of the unreconstructed surface. The Ni_4 cluster is formed by including the metal atoms nearest to the adsorbate, and the number of Ni atoms is the minimum required to represent the μ-bridging adsorption mode. The Ni_{14} cluster completes the Ni_4 cluster by surrounding its atoms with their first neighbors from the top layer. Although we realize that more Ni atoms (at least from the second layer for Ni_{14}) are necessary to model the metal surface and to obtain accurate adsorption energies [26], a cluster model which include the directly interacting metal atoms (even the Ni_4 cluster) should give reliable results for adsorption geometries. We will see below that the best adsorption mode calculated with the Ni_4 cluster remains valid with the Ni_{14} cluster. The cluster size especially affects the adsorption energy, as will be seen in the comparison of the adsorption on Ni_4 and Ni_{14} clusters. The geometry of the adsorbate is more sensitive to the adsorption mode (the number of metal atoms involved in the adsorption) rather than the cluster size. Therefore, the optimization of the adsorbate geometry will be performed using the Ni_4 cluster and transferred to the Ni_{14} cluster to obtain accurate adsorption energies. In Sections 5 and 6 dealing with the adsorption, we will discuss only the calculated properties (charge transfer, overlap population, density of states) obtained with the Ni_{14} cluster.

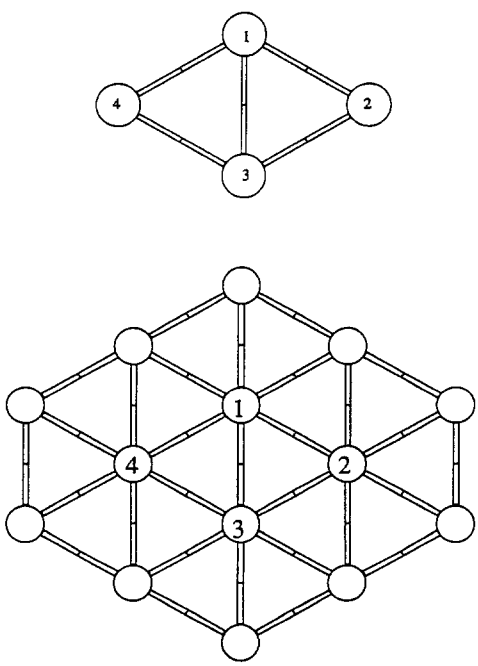

Fig. 2. The cluster models for the Ni(111) surface, Ni_4 and Ni_{14}.

During acetylene and ethylene adsorption on Ni(111), the C–C axis remains essentially parallel to the surface. The inclination of the C–C axis seems to be caused by the second-layer atoms, which are not included in our models. Therefore the adsorbate geometries are optimized using the C_{2v} symmetry as a constraint. The geometry of the cluster is fixed (Ni–Ni = 2.49 Å) and corresponds to that of a fragment extracted from the Ni(111) surface.

4. Bare Ni_4 and Ni_{14} clusters

Within the local spin density approximation, the ground state of a single nickel atom is d^9s^1 instead of the experimental d^8s^2 ground state [27]. The implementation of the ADF program does not allow the calculation of the separated J-states. However, we can calculate J-averaged low and high spin states and then the d^9s^1 (^3D) is more stable than $d^8s^2(^3F)$ [28]. Therefore, the reference for our calculations will be the nickel d^9s^1 state.

The ground state of our rhombic cluster (a fragment of the Ni(111) surface) is a triplet. The bonding energy of the cluster, relative to four Ni(d^9s^1) atoms, is 194 kcal mol^{-1}. This corresponds to an Ni–Ni bond strength of 39 kcal mol^{-1}. The Mulliken populations of the valence 3d, 4s and 4p orbitals are presented in Table 1, where the labels (1) and (2) correspond to the symmetrically different Ni atoms in the cluster (see Fig. 2).

Table 1
Mulliken populations and atomic charges in the Ni_4 and Ni_{14} bare clusters

Atom/cluster	d	s	p	Charge
Ni(1)				
Ni_4	8.87	1.04	0.11	−0.02
Ni_{14}	8.79	0.69	0.59	−0.07
Ni(3)				
Ni_4	8.89	0.79	0.30	+0.02
Ni_{14}	8.79	0.70	0.55	−0.04

Although there is a promotion of electrons from d to the s and p levels, in order to get a stabilizing interaction, the electronic structure of the Ni_4 cluster remains close to the d^9s^1 configuration. The energy band calculations for the nickel bulk structure gives a $d^{9.45}s^{0.55}$ configuration [29]. The Mulliken overlap populations of the Ni–Ni bonds in the cluster (0.23 for Ni(1)–Ni(2) and 0.14 for Ni(1)–Ni(3)) show that the bridge bond is the weakest bond of the cluster.

The modeling of an extended surface by a finite cluster always leads to an accumulation of electrons in atoms of low coordination [30]. Indeed, there is a transfer of 0.02 electrons from atom Ni(1) (coordination number 3) to atom Ni(2) (coordination number 2). However, this electron transfer due to the dissymmetry remains small and the electronic structures of the two atoms are very close.

For the Ni_{14} cluster, the presence of dense low-lying virtual orbitals caused some difficulties in convergence, and we had to use fractional electron occupations to force self-consistency. Therefore there are uncertainties in the electronic configuration and the spin state of the cluster. The calculated bonding energy, relative to Ni(d^9s^1) atoms, is 868 kcal mol^{-1}. The Ni–Ni bond strength, 30 kcal mol^{-1}, is still far from the bulk value of 17 kcal mol^{-1} [31].

The direct effect of the cluster size on the electronic structure is the promotion of electrons from both d and s orbitals towards the p orbitals, which therefore increases the participation of the p orbitals to the ground state (see Table 1). The overlap populations of the various Ni–Ni bonds are close (between 0.14 and 0.15). Therefore their bond strengths are close, in contrast to the Ni_4 cluster where the bridge bond is weak.

5. Acetylene adsorption

The optimization of the geometry of free acetylene gives C–C and C–H bond lengths of 1.20 and 1.08 Å, respectively. The agreement with experimental data is very satisfactory (C–C = 1.20 Å and C–H = 1.06 Å [32]).

During the interaction of acetylene or ethylene with a transition metal, donation and back donation processes take place. The donation involves a transfer of electrons from the π orbitals of the adsorbate to the metal unoccupied orbitals, whereas the back donation populates the π^* orbitals of the adsorbate with electrons from the occupied metal orbitals. This is the well-known Dewar–Chatt–Duncanson mechanism [33]. Both donation and back donation are attractive interactions. The repulsion (Pauli repulsion) is due to the interaction between the occupied orbitals of the adsorbate and the transition metal.

The results of the adsorption of acetylene are presented in Table 2. The geometry optimization is performed with the Ni_4 cluster. The C_2H_2/Ni_4 system is spin-triplet in both di-σ and μ-bridging orientations. In agreement with experiments [7], the best adsorption mode is μ-bridging. This result is found for both Ni_4 and Ni_{14} clusters. The difference between the adsorption energies of the two modes is not affected by the cluster size, 17 and 15 kcal mol^{-1} with Ni_4 and Ni_{14} clusters, respectively. The adsorption energy increases with the cluster size, from 37 to 50 kcal mol^{-1} (μ-bridging mode), but is still far from the estimated experimental value of 67 kcal mol^{-1} [34].

The first consequence of the donation and back donation processes is the weakening of the C–C bond strength (the bond length increases) and the formation of Ni–C bonds. There is a rehybridization of the carbon atoms toward the sp^3 configuration. The distortion of acetylene is stronger in the μ-bridging orientation, as can be seen from the values of the C–C bond length and C–C–H angle (Table 2). This is the consequence of strong adsorption. The difference of the total energies of acetylene

Table 2
Adsorption energies of C_2H_2 on Ni_4 and Ni_{14} clusters; the optimized geometries with the Ni_4 cluster: the height of the C–C axis from the surface in Å, the bond lengths and angles in Å and degrees, respectively; the Mulliken overlap populations (OP) correspond to the system C_2H_2/Ni_{14}

Adsorption mode	Adsorption energy	Height	C–C	Ni–C (OP)	C–C–H
μ-bridging					
Ni_4	37	1.27	1.51	1.89 Ni(1)–C (0.02)	119.5
Ni_{14}	50			1.93 Ni(2)–C (0.21)	
di-σ					
Ni_4	20	1.70	1.37	1.79 (0.25)	128
Ni_{14}	35				
Experiment	67[a]	1.37[e]	1.45–1.49[b], 1.50[c] 1.38–1.44[d], 1.44[e]	2.1[e]	120–130[d]

[a] Ref. [34]. [b] ELS, Ref. [36]. [c] LEED, Ref. [37]. [d] UPS, Ref. [38]. [e] Photoelectron diffraction, Ref. [7].

in the adsorbed and equilibrium geometries shows the magnitude of the distortion, a difference of 94 and 54 kcal mol^{-1} for μ-bridging and di-σ, respectively. The adsorption process is controlled by a balance between the energy required to relax the adsorbate on the surface and the energy gained by the formation of the adsorbate–substrate bonds. For acetylene in the μ-bridging orientation, the formation of the Ni–C bonds is large enough to compensate the energy required for the large deformation of the molecule on the surface. The optimized parameters (C–C, Ni–C and the height of the C–C axis from the surface) for the μ-bridging orientation are closer to the experimental values than the corresponding parameters for the di-σ orientation. The experimental value for the C–C bond length lies between 1.44 and 1.50 Å, according to the technique of evaluation. The overlap populations of the bonds between acetylene and the metal surface (Table 2) show that acetylene is attached by Ni(2) and Ni(4) in the μ-bridging orientation, and by Ni(1) and Ni(3) in the di-σ orientation.

The comparison of the net charges on C and H atoms before and after adsorption shows that the overall charge transfer is a back donation. The back donated electrons are mainly localized on the carbon atoms. Detailed analysis of the charge transfer shows individual donation and back donation processes which involve essentially the π and π^* orbitals of acetylene (see Table 3). For the μ-bridging adsorption on Ni_{14}, the back donation

Table 3
Charge transfers between acetylene frontier orbitals and the Ni_{14} cluster: donated electrons from π_σ and π, and backdonated electrons to π_σ^* and π_σ

	π_σ	π	π_σ^*	π^*
μ-bridging	0.65	0.72	1.12	0.49
di-σ	0.70	0.25	0.87	0.20

(1.61 electrons) is larger than the donation (1.37 electrons). Both processes are weaker for the di-σ adsorption, 1.07 and 0.95 electrons for the back donation and the donation, respectively.

Fig. 3 shows the density of states projected on π_σ, π, π_σ^* and π^* orbitals of acetylene. The positions of these orbitals for C_2H_2 in the geometry of adsorption are also indicated to show how the states are shifted down in energy by the adsorption. The energies of the C_2H_2 orbitals increase in the order $\pi_\sigma < \pi < \pi_\sigma^* < \pi^*$. Therefore the frontier orbitals are π (HOMO) and π_σ^* (LUMO). The π_σ mixed lone pair is more stable than the π orbital. In contrast, previous theoretical studies (extended Huckel [15] and ab-initio [13,14]) have found the reverse order, π being more stable than π_σ. The discrepancy can be attributed to the polarization functions which are missing in the previous ab-initio results. With the Gaussian program, the STO-3G basis set gives the order $\pi < \pi_\sigma$, whereas the 6-31G** basis set gives the order $\pi_\sigma < \pi$. All

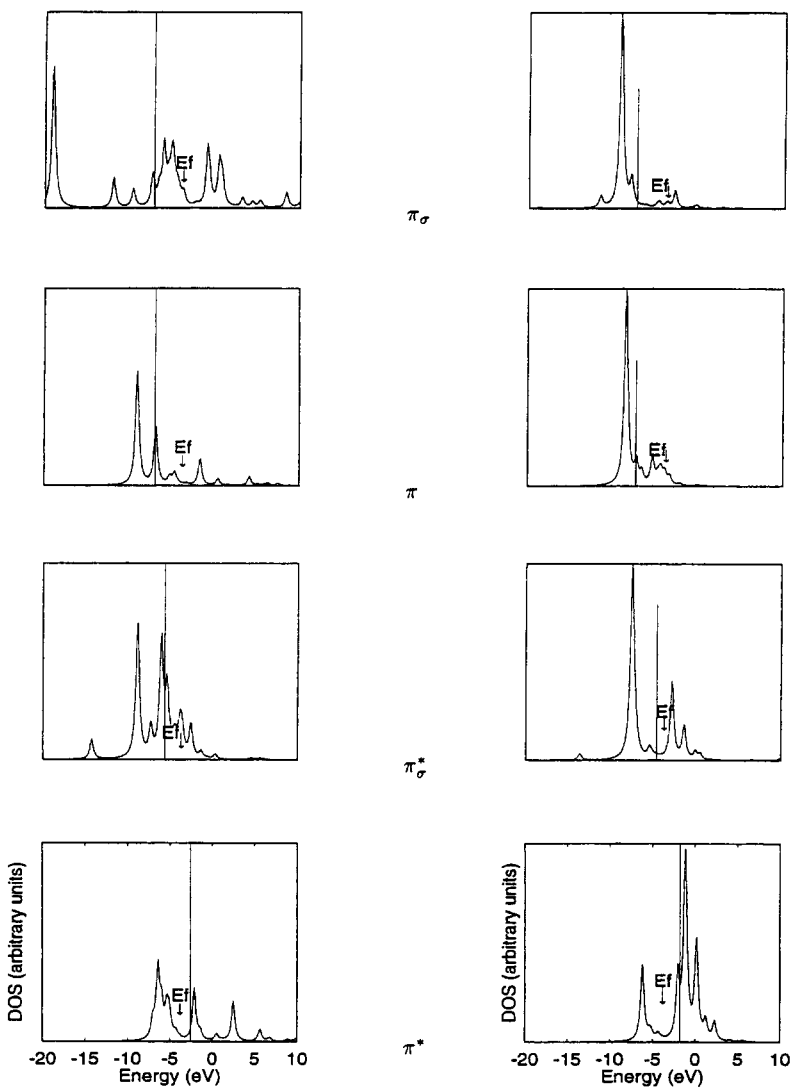

Fig. 3. Density of states projected on the frontier orbitals of acetylene (π_σ,π,π^*_σ and π^*). The stick marks indicate the position of the corresponding states (for acetylene in the adsorbed geometry) in the absence of interaction with the metal. The Fermi level (E_F) is indicated by an arrow. The DOS curves are broadened by Lorentzian functions of 0.25 width factor.

the projected density of states are broadened over a large energy range due to the overlap with the cluster orbitals. Bonding contributions appear below the Fermi level (E_F) and correspond to donation (π_σ,π) and back donation (π^*_σ, π^*). The more the orbital is shifted downwards, the stronger the electron transfer. This correlation can be seen in Table 3, where the amounts of transferred electrons are presented. It is in the behavior of π and π^*_σ orbitals that we find the largest electronic effects due to the adsorption. In the μ-bridging adsorption mode, the electron transfer is larger for

π and π_σ^* orbitals and the corresponding DOS are shifted further down in energy than the π_σ and π^* orbitals. We notice from Table 3 that the main difference between the μ-bridging and di-σ orientations is due to the contribution of the π orbital (donation). The large donation in the μ-bridging orientation involves the d orbitals of the metal surface, as can be seen from the Mulliken overlap populations of the π orbital with the s, p and d orbitals of Ni(1)–(4) atoms of the Ni_{14} cluster (Table 4). Although there is an antibonding interaction with the s states in the di-σ orientation, the difference between the two adsorption modes is essentially due the interaction with the d states.

The large donation in the μ-bridging orientation populates the antibonding orbitals of the metal surface. The consequence is better seen in the decrease of the overlap population of the Ni(1)–Ni(3) bridge bond, it drops from 0.15 (bare cluster) to 0.04. The effect is smaller in the di-σ orientation, the overlap population of the bridge bond is 0.11.

Upon adsorption, the acetylene triple bond is significantly weakened. The bond length increases from 1.20 to 1.51 Å (μ-bridging) and 1.37 Å (di-σ). The C–C overlap population drops from 0.89 (gas phase) to 0.12 (μ-bridging) and 0.34 (di-σ). Both donation (depopulation of π_σ and π) and back donation (population of π_σ^* and π^*) contribute to this weakening. The C–H bond character is not affected by the adsorption. The C–H bond lengths, 1.03 Å for μ-bridging and 1.11 Å for di-σ, remain close to the gas-phase value of 1.08 Å.

From these considerations, C–C bond cleavage seems to be more favourable than C–H bond cleavage. Indeed Zhu and White [1] suggested from TPSSIMS experiments that C–C cleavage as the first step in acetylene decomposition on Ni(111). The C–C cleavage starts at 190 K, whereas C–H cleavage starts at 260 K. Our calculations suggest that the μ-bridging orientation is suitable for the activation of the C–C bond.

Table 4
Overlap populations of acetylene π orbital with Ni_{14} orbitals (arbitrary units)

	s	p	d	Total
μ-bridging	0.06	0.04	0.20	0.30
di-σ	−0.01	0.04	0.00	0.03

The concept that emerges from our calculations is that the best adsorption mode (μ-bridging) is characterized by a large electron transfer in both directions, $C_2H_2 \rightarrow$metal and metal$\rightarrow C_2H_2$. As a consequence the adsorption is very strong, to the detriment of the stability of both the C_2H_2 molecule and the metal surface. The bonds within the two entities become weaker.

6. Ethylene adsorption

The calculated geometry for free ethylene is very close to the experimental data [32]: C–C = 1.34 Å, C–H = 1.06 Å and H–C–H = 117.0°. The experimental values are 1.34 Å, 1.09 Å and 117.8°, respectively.

For the adsorption study, we follow the same procedure as before. The geometry of adsorbed ethylene is optimized with the Ni_4 cluster and transferred to the Ni_{14} cluster. The molecular properties for adsorbed ethylene are presented in Table 5. The C_2H_4/Ni_4 system is spin-triplet in both di-σ and μ-bridging orientations. In agreement with experimental results [7], the best adsorption mode for ethylene is di-σ. This result is again found for the two clusters, Ni_4 and Ni_{14}. The calculated adsorption energy for the di-σ orientation is 13 kcal mol^{-1}. The available experimental value, 12 kcal mol^{-1} [35], is rather attributed to the physisorption state. The calculated C–C bond length (for di-σ mode), 1.49 Å, is very close to the experimental value determined by HREELS [9], 1.47 Å, but is far from the value determined using scanned-energy mode photoelectron diffraction [7], 1.60 Å. However, this later technique gives a value for the height of the C–C axis from the surface of 1.90 Å, which is very close to our calculated value of 1.89 Å. On the other hand, when comparing the C–C bond lengths of acetylene and ethylene in their best adsorption modes (1.51 Å for C_2H_2 and 1.49 Å for C_2H_4), the value for acetylene appears abnormally long. However, when considering the same adsorption mode, the C–C bond length of acetylene indeed

Table 5
Adsorption energies of C_2H_4 on Ni_4 and Ni_{14} clusters; the optimized geometries with the Ni_4 cluster: the height of the C–C axis from the surface in Å, the bond lengths and angles in Å and degrees, respectively; the Mulliken overlap populations (OP) correspond to the system C_2H_4/Ni_{14}

Adsorption mode	Adsorption energy	Height	C–C	Ni–C (OP)	H–C–C
μ-bridging					
Ni_4	−18	1.81	1.58	2.27 (0.15)	113.0
Ni_{14}	3				
di-σ					
Ni_4	−4	1.89	1.49	1.95 (0.21)	114.5
Ni_{14}	13				
Experiment	>12[a]	1.90[c]	1.47[b], 1.60[c]		

[a] From molecular beam measurements, Zuhr and Hudson [35] concluded that the value they found for the adsorption of ethylene on Ni(111), 12 kcal mol^{-1}, refers to a physisorbed state, possibly on top of a chemisorbed layer.
[b] HREELS, Ref. [9].
[c] Photoelectron diffraction, Ref. [7].

Table 6
Charge transfers between ethylene frontier orbitals and the Ni_{14} cluster: donated electrons from π and backdonated electrons to π^*

	π	π^*
di-σ	0.65	0.72
μ-bridging	0.59	0.04

Table 7
Overlap populations of ethylene π and π^* orbitals with Ni_{14} orbitals (arbitrary units)

	s	p	d	Total
π^*				
di-σ	0	0.04	0.06	0.10
μ-bridging	0	0	0.01	0.01
π				
di-σ	0.04	0.05	0.02	0.11
μ-bridging	0.03	0.05	0.02	0.10

remains smaller than that of ethylene: 1.51 versus 1.58 Å for μ-bridging, and 1.37 versus 1.49 Å for di-σ. Therefore the weakening of the C–C bond of ethylene due to adsorption is smaller than that of acetylene. TPSSIMS experiments [1] have shown that the C–H bond cleavage is the first step in ethylene decomposition: ethylidyne ($C-CH_3$) and acetylene were found at 200 K, whereas acetylide (C–CH) and methylidyne (CH) were found at a higher temperature (300 K). However, our calculations do not show a weakening of the C–H bond. The C–H bond lengths, 1.10 Å for di-σ and 1.13 Å for μ-bridging, remain close to the gas-phase value of 1.10 Å.

Table 6 shows the amount of electron transfers, and Table 7 shows the overlap populations of ethylene frontier orbitals (π and π^*) with s, p and d orbitals of Ni(1)–(4) atoms of the Ni_{14} cluster. The π orbital interacts mainly with the s and p orbitals, whereas the π^* orbital interacts with p and d orbitals. The main difference between di-σ and μ-bridging orientations is due to the contribution of the π^* orbital. This orbital does not overlap with the metal orbitals in the μ-bridging orientation, and therefore the back donation is not significant. The projected DOS on π and π^* (Fig. 4) corroborate this trend. While π^* is shifted down below the Fermi level in the di-σ orientation, most of its density is shifted above the Fermi level in the μ-bridging orientation.

Finally, the difference of ethylene and acetylene adsorption energies and geometries seems to be due to the presence on acetylene of two active orbitals which allow extra donation and back donation, as can be seen from the comparison of charge transfers (see Tables 3 and 6).

7. Conclusion

In this study, we have investigated the adsorption of acetylene and ethylene on Ni(111) using

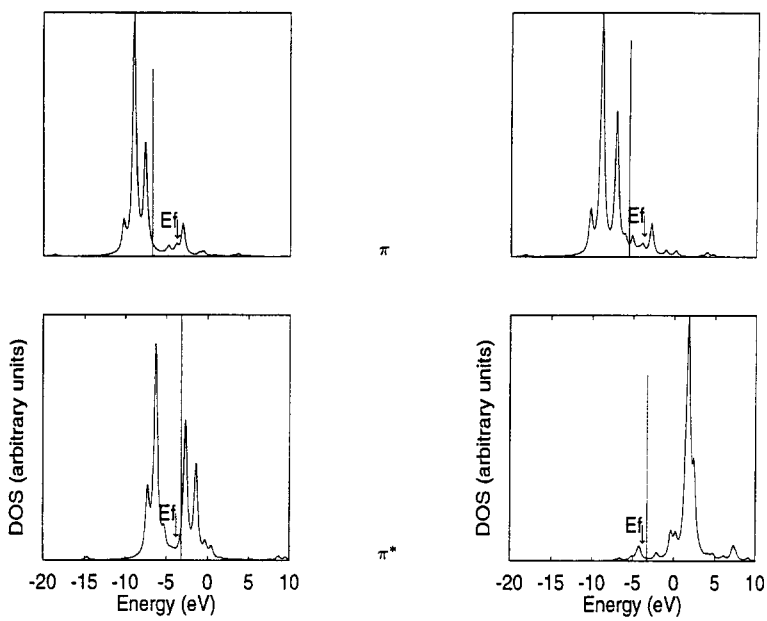

C_2H_4 (di-σ)/Ni_{14} C_2H_4 (μ-bridging)/Ni_{14}

Fig. 4. Density of states projected on the frontier orbitals of ethylene (π and π^*). The stick marks indicate the position of the corresponding states (for ethylene in the adsorbed geometry) in the absence of interaction with the metal. The Fermi level (E_F) is indicated by an arrow. The DOS curves are broadened by Lorentzian functions of 0.25 width factor.

Ni_4 and Ni_{14} clusters as models. Despite the limited size of the clusters, interesting features of the adsorbate–metal surface were determined, i.e. adsorption energies, adsorbate geometries and electronic factors governing the adsorption process. Therefore the cluster approximation remains a useful tool to access the surface chemical reactivity.

The calculations support the picture of strongly distorted adsorbates suggested by various surface experimental studies [7,9,36–38]: there is a rehybridization of the carbon atoms toward the sp^3 configuration and a lengthening of the C–C bonds. The best adsorption modes are μ-bridging and di-σ for acetylene and ethylene, respectively. In these orientations the overlap between the adsorbate frontier orbitals and the metal cluster orbitals is important and the donation–back donation processes are very large. For both adsorbates the back donation is stronger than the donation and leads to negatively charged species on the surface. These two processes contribute to the weakening of the C–C bond, and for acetylene C–C bond cleavage seems to be the first step in the decomposition reaction. The best adsorption mode is related to the number of atoms involved in the adsorbate–substrate interaction, and therefore is the same for Ni_4 and Ni_{14} clusters. The cluster size affects mainly the adsorption energy, which increases with the size.

Acknowledgements

We would like to thank the theoretical group of the Free University of Amsterdam for the use of the ADF program. This work was supported by the Eindhoven University of Technology. We kindly acknowledge the computational resources allocated from the National Computing Facilities (NCF) Foundation under project SC-183.

References

[1] X.-Y. Zhu and J.M. White, Surf. Sci. 214 (1989) 240.
[2] J.E. Demuth, Surf. Sci. 69 (1977) 365.
[3] J.E. Demuth and H. Ibach, Surf. Sci. 78 (1978) 238.
[4] M.G. Cattania, M. Simonetta and M. Tescari, Surf. Sci. 82 (1979) 615.
[5] J.E. Demuth, Surf. Sci. 76 (1978) 603.
[6] L. Hammer and K. Muller, Prog. Surf. Sci. 35 (1991) 103.
[7] S. Bao, Ph. Hofmann, K.-M. Schindler, V. Fritzsche, A.M. Bradshaw, D.P. Woodruff, C. Casado and M.C. Asensio, J. Phys. Condens. Matter 6 (1994) L93.
[8] P. Geurts and A. van der Avoird, Surf. Sci. 102 (1981) 185.
[9] H. Ibach and S. Lehwald, J. Vac. Sci. Technol. 18 (1981) 625.
[10] R.G. Carr, T.K. Sham and W.E. Eberhardt, Chem. Phys. Lett. 113 (1985) 63.
[11] A. Gavezzotti, E. Ortoleva and M. Simonetta, J. Chem. Soc., Faraday Trans. I 78 (1982) 425.
[12] H. Kobayashi, S. Yoshida and M. Yamaguchi, J. Phys. Chem. 87 (1983) 1140.
[13] H. Kobayashi, H. Teramae, T. Yamabe and M. Yamaguchi, Surf. Sci. 141 (1984) 580.
[14] K. Hermann and M. Witko, Surf. Sci. 337 (1995) 205; A. Clotet and G. Pacchioni, Surf. Sci. 346 (1996) 91; H. Sellers, J. Phys. Chem. 94 (1990) 8329.
[15] J. Silvestre and R. Hoffmann, Langmuir 1 (1985) 621.
[16] X. Xu, N.Q. Wang and Q.E. Zhang, J. Mol. Struct. 247 (1991) 93.
[17] X.S. Feng and J.C. Tang, Catal. Lett. 20 (1993) 141.
[18] M. Weinelt, W. Huber, P. Zebisch, H.-P. Steinbruck, M. Pabst and N. Rosch, Surf. Sci. 271 (1992) 539; U. Gutdeutsch, U. Birkenheuer, E. Bertel, J. Cramer, J.C. Boettger and N. Rosch, Surf. Sci. 345 (1996) 331.
[19] J.-F. Paul and P. Sautet, J. Phys. Chem. 98 (1994) 10906.
[20] V. Maurice and C. Minot, Langmuir 5 (1989) 734.
[21] E.J. Baerends, D.E. Elis and P. Ros, Chem. Phys. 2 (1973) 41; P.M. Boerrigter, G. te Velde and E.J. Baerends, Int. J. Quantum Chem. 33 (1988) 87; E.J. Baerends and P. Ros, Int. J. Quantum Chem.: Quantum Chem. Symp. 12 (1978) 169.
[22] S.H. Vosko, L. Wilk and M. Nusair, Can. J. Phys. 58 (1980) 1200.
[23] A.D. Becke, Phys. Rev. A 38 (1988) 3098; ACS Symp. Series 394 (1989) 165.
[24] J.P. Perdew, Phys. Rev. B 33 (1986) 8822.
[25] J.G. Snijders and E.J. Baerends, Mol. Phys. 36 (1978) 1789; 38 (1979) 1909.
[26] M.C. Zonnevylle, J.J.C. Geerlings and R.A. van Santen, J. Catal. 148 (1994) 417.
[27] C.E. Moore, Atomic Energy Levels (National Bureau of Standards, Washington DC, 1952).
[28] H. Burghgraef, A.P.J. Jansen and R.A. van Santen, J. Chem. Phys. 98 (1993) 8810; 101 (1994) 11012.
[29] A. Clark, The Theory of Adsorption and Catalysis (Academic Press, New York, 1970) p. 176.
[30] P. Sautet and J.-F. Paul, Catal. Lett. 9 (1991) 245.
[31] R.C. West (Ed.), Handbook of Chemistry and Physics (CRC, Cleveland, 1986).
[32] W.J. Hehre, L. Radom, P.V.R. Schleyer and J.A. Pople, Ab-initio Molecular Theory (Wiley, New York, 1986).
[33] M.J.S. Dewar, Bull. Soc. Chim. France C 71 (1950) 18; J. Chatt and L.A. Duncanson, J. Chem. Soc. London (1953) 2939.
[34] G.C. Bond, Catalysis by Metals (Academic Press, New York, 1962).
[35] R.A. Zuhr and J.B. Hudson Surf. Sci. 66 (1977) 405.
[36] J.E. Demuth and H. Ibach, Surf. Sci. 85 (1979) 365.
[37] G. Casalone, M.G. Cattania, F. Merati and M. Simonetta, Surf. Sci. 120 (1982) 171.
[38] J.E. Demuth, Surf. Sci. 84 (1979) 315.